

## Enhancing power distribution network operational resilience to extreme wind events

Donaldson, Daniel L.; Ferranti, Emma J.S.; Quinn, Andrew D.; Jayaweera, Dilan; Peasley, Thomas; Mercer, Mark

DOI:  
[10.1002/met.2127](https://doi.org/10.1002/met.2127)

License:  
Creative Commons: Attribution (CC BY)

*Document Version*  
Publisher's PDF, also known as Version of record

*Citation for published version (Harvard):*  
Donaldson, DL, Ferranti, EJS, Quinn, AD, Jayaweera, D, Peasley, T & Mercer, M 2023, 'Enhancing power distribution network operational resilience to extreme wind events', *Meteorological Applications*, vol. 30, no. 2, e2127. <https://doi.org/10.1002/met.2127>

[Link to publication on Research at Birmingham portal](#)

### General rights

Unless a licence is specified above, all rights (including copyright and moral rights) in this document are retained by the authors and/or the copyright holders. The express permission of the copyright holder must be obtained for any use of this material other than for purposes permitted by law.

- Users may freely distribute the URL that is used to identify this publication.
- Users may download and/or print one copy of the publication from the University of Birmingham research portal for the purpose of private study or non-commercial research.
- User may use extracts from the document in line with the concept of 'fair dealing' under the Copyright, Designs and Patents Act 1988 (?)
- Users may not further distribute the material nor use it for the purposes of commercial gain.

Where a licence is displayed above, please note the terms and conditions of the licence govern your use of this document.

When citing, please reference the published version.



### Take down policy

While the University of Birmingham exercises care and attention in making items available there are rare occasions when an item has been uploaded in error or has been deemed to be commercially or otherwise sensitive.

If you believe that this is the case for this document, please contact [UBIRA@lists.bham.ac.uk](mailto:UBIRA@lists.bham.ac.uk) providing details and we will remove access to the work immediately and investigate.

## RESEARCH ARTICLE

# Enhancing power distribution network operational resilience to extreme wind events

Daniel L. Donaldson<sup>1</sup>  | Emma J.S. Ferranti<sup>1</sup>  | Andrew D. Quinn<sup>1</sup>  |  
Dilan Jayaweera<sup>1</sup>  | Thomas Peasley<sup>2</sup> | Mark Mercer<sup>2</sup>

<sup>1</sup>School of Engineering, University of Birmingham, Birmingham, UK

<sup>2</sup>Electricity North West (ENWL), Manchester, UK

## Correspondence

Emma Ferranti, University of Birmingham, Birmingham, B15 2TT, UK.  
Email: [e.ferranti@bham.ac.uk](mailto:e.ferranti@bham.ac.uk)

## Funding information

Engineering and Physical Sciences Research Council, Grant/Award Number: EP/R007365/1; EPSRC Impact Acceleration grant awarded by the University of Birmingham

## Abstract

Extreme weather events can cause significant damage to power distribution network infrastructure, often resulting in power outages. Distribution Network Operators (DNOs) are faced with the challenging task of responding to these outages in real time while maintaining a resilient grid. Our paper presents an innovative approach to alert operators about the potential risk associated with upcoming extreme weather through a normalized fragility curve. The uniqueness of the curve is the ability to capture regional differences across a DNO's territory while presenting operators with a means of setting unified risk thresholds. This can support a proactive response and allow the staging of necessary resources to minimize the threat posed by such events. Our approach captures the changes in failure probability associated with differing wind regimes and demonstrates the benefit of sub-regional meteorological information. The proposed approach is demonstrated for wind events using 20 years of historical fault records from a DNO in the United Kingdom (UK). While its efficacy is demonstrated for windstorms in the UK, the approach could be applied globally to develop normalized fragility curves for other types of seasonal extreme weather events such as snowstorms, hurricanes, or linked hazards such as wildfires. The approach can also facilitate an understanding of how infrastructure may operate under future climate conditions, supporting proactive adaptation.

## KEYWORDS

climate adaptation, infrastructure resilience, weather impact

## 1 | INTRODUCTION

The electric power distribution network underpins infrastructure such as water, communications and transportation. “As electricity is decarbonised and other sectors increasingly become electrified, the provision of a reliable

supply becomes ever more important to society and the economy” (Jaroszweski et al., 2021, p. 87). Shield et al. (2021) performed an assessment of major power outages in the United States from 2003 to 2017 and found weather responsible for 50% of all events, affecting 83% of customers, with a median restoration cost during a major

This is an open access article under the terms of the [Creative Commons Attribution](https://creativecommons.org/licenses/by/4.0/) License, which permits use, distribution and reproduction in any medium, provided the original work is properly cited.

© 2023 The Authors. Meteorological Applications published by John Wiley & Sons Ltd on behalf of the Royal Meteorological Society.

storm of ~\$12 million. For DNOs weather-related faults can comprise a large portion of distribution infrastructure outages, with one DNO reporting 17% of annual faults caused by Weather and Environment or Flooding (on average in the 5 years from 2015) (ENWL, 2021), and DNO groups in the United Kingdom spending £151m to improve resilience in 2019–2020 alone (OFGEM, 2020). Examples of weather events causing disruption of the electricity distribution network include flooding (Ferranti et al., 2017) and storms (BEIS, 2021). DNOs are faced with the challenging task of responding to such events in near-real time and maintaining grid operation.

In November–December 2021, some areas of the UK experienced “the equivalent of almost two years’ worth of overhead line faults in just one 12-hour period” (Scottish and Southern Electricity Networks, 2021) as Storm Arwen resulted in power outages for around one million customers, leaving some without power for up to 13 days (BEIS, 2022a). As a result, the UK Energy Emergencies Executive Committee (E3C) carried out a review to consider the need to address system resilience (BEIS, 2021). One key finding of the interim report states that “All DNOs should review their severe weather escalation plans to ensure that all relevant factors, including wind direction, are taken into consideration” (BEIS, 2022a, p. 12). Giving DNOs more information about the potential risk posed to the power system by upcoming extreme weather can support a proactive response and allow the staging of necessary resources, such as additional maintenance teams or incident management teams, to minimize the threat posed by such events, thereby enhancing resilience. This paper focuses on the effects of windstorms on power distribution network resilience and provides insight enabling transfer learning for other weather phenomena.

High wind speeds can cause failures within the distribution network in two key ways: (1) Application of force directly to assets themselves resulting in failure (which may be worsened by the build-up of ice during a winter storm), or (2) failure due to flying debris or vegetation that comes into contact with the assets (BEIS, 2022b). The failure duration can be momentary or sustained and thereby requiring repair or further action prior to restoration of service (IEEE, 2012). As the energy sector is decarbonized and the dependence of society on reliable electricity grows (Jaroszweski et al., 2021), the ability to proactively anticipate these faults due to high wind gusts will be of increasing global importance. Fragility curves provide a useful means of achieving this aim by representing the likelihood of failure of a specific piece of infrastructure under a range of conditions and have been applied to electric power systems for a variety of extreme events including earthquakes (Lagos et al., 2020;

Zareei et al., 2016) and windstorms (Dunn et al., 2018; Murray & Bell, 2014; Panteli et al., 2017; Wilkinson et al., 2022).

Jeong and Elnashai (2007) group methods to develop fragility curves into four categories: (1) Analytical approaches which seek to use structural simulation models to reflect the likelihood of failure as used by Panteli et al. (2017) and Zareei et al. (2016); (2) Empirical approaches which rely on large amounts of historical failure data such as those used by Murray and Bell (2014) and Dunn et al. (2018); (3) Judgemental approaches which form probabilities based on expert opinions; and (4) Hybrid approaches which seek to combine two or more approaches in an attempt to overcome the limitations of a single method (“scarcity of observational data, subjectivity of judgmental data and modeling deficiencies of analytical procedures”) (Jeong & Elnashai, 2007, p. 1239). A critical determinant of the most suitable approach when developing a fragility curve is data availability. Often sufficient historical information is unavailable, requiring the development of analytical approaches or expert judgement. Experimental methods which rely on controlled environments to evaluate the failure of components can also be used to generate data, but are often impractical due to the expense of testing (Schultz et al., 2010). In this work, an empirical approach is taken given the availability of extensive fault records of wind-related distribution equipment failures.

When designing infrastructure, structural design codes and standards dictate the minimum wind loading that each structure should be designed to withstand. Examples of such standards include BS EN 1991-1-4:2005 “Eurocode 1. Actions on structures—General actions—Wind actions” (BSI, 2005) in the United Kingdom, and ASCE/SEI 7–10 in the United States (ASC, 2013). As a result of design codes and standards, the designed wind resilience of power system infrastructure can differ based on the anticipated wind regimes for a given region, causing the likelihood of failure at a specific wind speed to differ regionally. A historical example of this can be seen in damage to buildings and structures in the UK where “damage starts at about 15 m/s in the south and 17.5 m/s in the north” (Cook, 1985, p. 51). The likelihood of such failures is associated with a variety of factors including the wind regimes in a given area, the surrounding land cover and the design of the electrical assets themselves. Each factor plays a critical role in the susceptibility to faults and is subject to change as the power system is modernized and as global climate may alter wind regimes (Maisey et al., 2019; Scott Hosking et al., 2018) and vegetation growing seasons (Northern Powergrid, 2010). Although DNO work is ongoing to develop new fragility curves (Troshka, 2022), existing power system fragility

curve approaches often utilize a single curve to reflect a given service area (Dunn et al., 2018; Murray & Bell, 2014). While fragility curves can provide a useful means of informing grid operators of the potential risk of an upcoming storm, the spatial variance in the land cover, orography, and asset design means that in addition to spatial variance in wind speed, there is also a spatial variance in fragility. Therefore, the application of a singular fragility curve is likely to be insufficient, overestimating fragility in some areas while underestimating fragility in others. Wilkinson et al. (2022) present a regional analysis to develop fragility curves for specific regions, but this can potentially create difficulty in creating consistent thresholds for use and interpretation by grid operators.

The contributions from this work include: (1) A regional weather-based normalization model to produce fragility curves using extreme value theory; and (2) An innovative methodology to use the proposed regional weather-based normalization model for power distribution system infrastructure to enable more effective threshold setting while maintaining interpretability for grid operators. Based on the findings of this investigation, this study argues the need for DNOs to calculate regional fragility models to better monitor regional performance across their service territory. The findings also reflect seasonal and directional variance in the cumulative amount of wind-related failures, demonstrating that exposure varies across the season and wind direction, supporting the recent finding by BEIS (BEIS, 2022a). The significance of these results is assessed within the context of future climate projections and the process of climate adaptation within the UK.

## 2 | DISTRIBUTION NETWORK FRAGILITY FUNCTION METHODOLOGY

A fragility function enables DNOs to look at the upcoming weather forecast and anticipate the number of faults that might be expected across their service area. A traditional fragility curve has bounds of zero to one and reflects the probability that a given asset will fail, given a specific loading upon that asset (in this case wind speed) (Schultz et al., 2010). However, a single DNO has a significant number of infrastructure assets. For example, a DNO may have hundreds or thousands of kilometers of overhead distribution lines and associated line equipment. Hence, rather than calculating the probability that a singular asset fails, the fragility function is defined as the anticipated number of faults per a given distance of the overhead distribution line. A distance metric is

chosen to normalize faults rather than an area-based measure as the focus is on the amount of distribution infrastructure rather than the size of the region. This choice of metric also enables comparison with the fragility functions developed in this work to those developed by Dunn et al. (2018) and Murray and Bell (2014). However, Murray focuses on transmission-level faults which are not directly comparable as transmission infrastructure is more robust. Furthermore, Dunn et al. (2018) group nearby faults by windstorms rather than individual hours, so care should be taken when comparing the magnitude of faults across studies.

### 2.1 | Standard fragility function

To calculate the fragility function, three pieces of information are necessary: (1) Historical wind speed. (2) The number of faults associated with that wind speed. (3) The distance of the overhead distribution line exposed to that particular wind speed. The function which provides the calculated number of faults at each wind speed for a given region is as follows:

$$N_p(v) = \frac{N_f(v) d}{N_h(v) L}, \quad (1)$$

where  $N_p$  is the predicted number of faults at a given maximum wind gust  $v$ ;  $N_f$  is the number of faults;  $N_h$  is the number of hours of exposure;  $d$  is the desired representative distance (in km) for the resulting fault prediction, and  $L$  is the total overhead distribution line exposed (measured in km) exposed to a specific wind speed (grouped by region) used to normalize the fault rate for this analysis. As the aim of this methodology is to examine the relative variability in performance across regions rather than directly assessing the accuracy of the fragility curve, a backcasting methodology is not included. However, when applying a fragility curve to anticipate the number of faults, assessing the accuracy using an out-of-sample test period is recommended to anticipate the performance.

### 2.2 | Regional weather normalized fragility function

In order to account for differences in wind profile and design standards across the sub-regions of a utility, the wind speed for that region  $v = v_1, v_2, \dots, v_n$  is normalized to fall within the range [0,1] via min-max normalization (Han et al., 2012):

$$v'_i = \frac{v_i - v_{\min}}{v_{\max} - v_{\min}}, \quad (2)$$

where  $v'_i$  and  $v_i$  reflect the normalized and actual wind gust at the time  $i$ ;  $v_{\min}$  is the minimum wind gust; and  $v_{\max}$  is the maximum wind gust which must be calculated for each region. One approach would be to take  $v_{\max}$  as the maximum observed gust for each region. However, this would introduce an inconsistency in the scaling due to the unknown probability of the observed gust occurring and the likelihood that these probabilities were different in each of the regions. Therefore, an estimate of  $v_{\max}$  with a known probability of occurrence is required. A variable is used for the minimum wind gust to allow the exclusion of wind-related faults below a certain wind threshold if desired. However, a  $v_{\min}$  value of 0 is recommended for most cases to maintain the interpretability of the fragility function.

The value of  $v_{\max}$  for a given region can be calculated by fitting a distribution to the historical observations and calculating the return period using Extreme Value Theory. Extreme values of wind are commonly expressed in terms of  $v_T$  which reflect the maximum wind gust that is exceeded, on average once every  $T$  year (Palutikof et al., 1999). Palutikof et al. (1999) summarize the numerous methods present to do this in the literature. A commonly used method to estimate the parameters of extreme wind speeds is Gumbel's method (Cook, 1985; Gumbel, 1958). Linear regression is often used to identify a least-squares fit through the observed values yielding the extreme wind speeds for each return period of interest. However, this method results in biased estimates, especially at higher wind speeds (Cook, 1985; Palutikof et al., 1999). To overcome this deficit, the Lieblein BLUE (best linear unbiased estimators) method, proposed in (Lieblein, 1974) and detailed in (Cook, 1985) is used to determine the plotting positions for this paper. The steps are as follows:

1. Select the annual maximum observed wind gust ( $x$ ) at each station from the historical observations and arrange in ascending fashion  $\forall x \in \mathcal{X}$  where  $N$  is the number of years of historical data

$$x_1 \leq x_2 \leq \dots \leq x_N. \quad (3)$$

2. For each year, square the maximum annual gust speed such that

$$x'_m = x_m^2. \quad (4)$$

3. Copy the values of  $A(m)$  and  $B(m)$  from the Lieblein BLUE Lookup table given in (Cook, 1985, pp. 320–323)

4. Check that the BLUE values have been correctly copied by comparing the sum of  $A(m)$  and  $B(m)$  with the checksum values in the lookup table.
5. Calculate the mode  $U_{x'}$ :

$$U_{x'} = \sum_{m=1}^N A(m)x'(m). \quad (5)$$

6. Calculate the dispersion  $1/a_{x'}$

$$1/a_{x'} = \sum_{m=1}^N B(m)x'(m). \quad (6)$$

7. Calculate the Wind Gust for the Return period of interest

$$v_R = \left( U_{x'} - (1/a_{x'}) \ln \left( -\ln \left( 1 - \frac{1}{R} \right) \right) \right)^{0.5}, \quad (7)$$

where  $R$  is the return period in years.

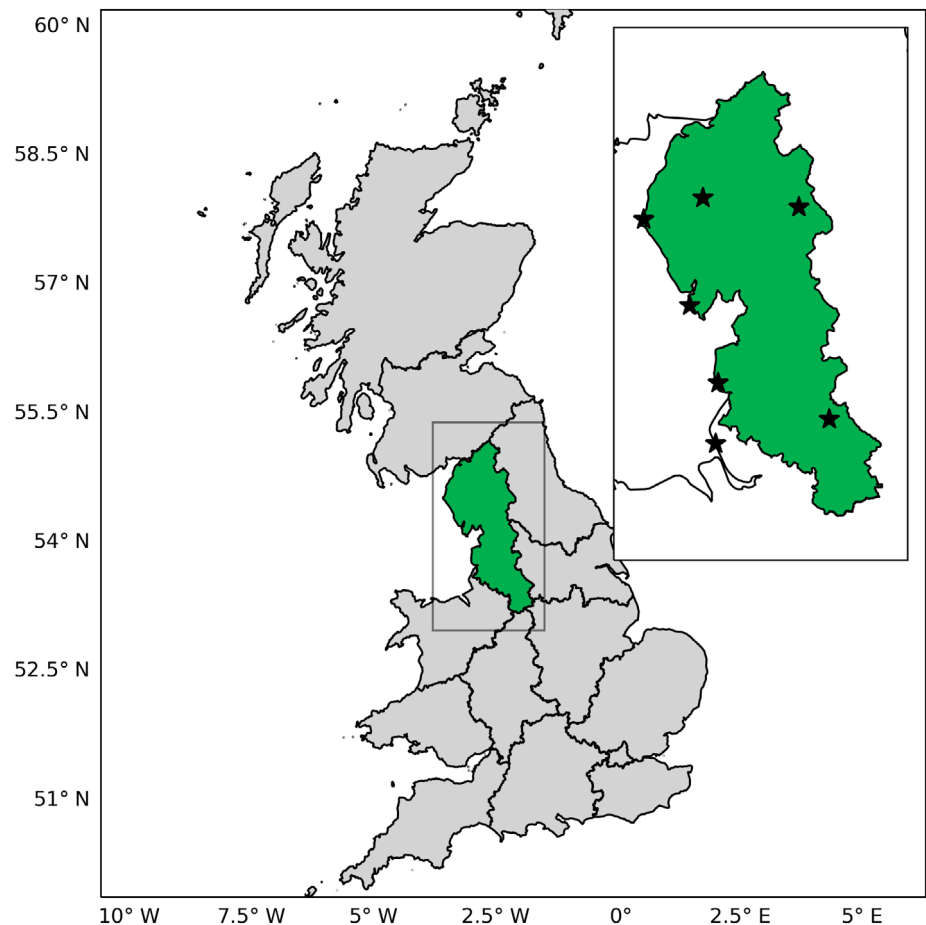
The approach selected for use in this paper carries the overall benefit of minimizing the number of decision variables that must be calculated by a grid operator in order to identify the extreme values. Other methods such as the  $r$ -largest values, method of independent storms (MIS) or the peak over the threshold (POT) have also been proposed in the literature and could also be used to generate  $v_R$  but require the selection of several additional decision variables (Palutikof et al., 1999). When using annual maxima, the minimum length of data that should be used is 20 years. Once the extreme value  $v_R$  has been calculated, the return period can be selected for use in developing the normalized fragility curve. While longer return periods can be used, the fragility functions will be subject to significant volatility based on hours with extreme winds that occur infrequently. The proposed methodology addresses this by excluding values exceeding  $v_R$  from the creation of the fragility curve. The resulting normalized wind speeds from (2) are then substituted into (1) to produce normalized fragility functions for each station.

### 3 | NORTHWEST ENGLAND CASE STUDY

#### 3.1 | Study area

In Great Britain, the electric distribution network is maintained by 14 DNOs managed by 6 groups

**FIGURE 1** Location of weather stations used in the analysis (shown as stars) and Great Britain Distribution Network Operators (DNOs) with Electricity North West service area (shown in green). DNO boundaries obtained from (National Grid Electricity System Operator, 2020).



(OFGEM, 2020) (Figure 1). This analysis focuses on the service area of one of these DNOs, located in the north-west of England; Electricity North West (ENWL). North-west England is exposed to westerly maritime masses that bring mild, moist air from across the Atlantic Ocean and is one of the wettest places in the United Kingdom (UK) (Met Office, 2016). As the region occupies the coast, it is particularly exposed to strong winds associated with the passage of deep areas of low pressure from the Atlantic (Met Office, 2016). As a result of these depressions, wind speeds and associated wind gusts are strongest during the winter months (December–February).

In the past decade, this area has experienced several major storms bringing heavy winds, rainfall and flooding. Examples include winds on February 12, 2014 (Met Office, 2014) and Storm Desmond on December 4–5, 2015 (Ferranti et al., 2017). Wind on February 12, 2014 led the Met Office to issue a “Red Warning,” for wind and left 100,000 homes and businesses without power (Met Office, 2014). Storm Desmond adversely impacted regional infrastructure, leading to cascading failures of power, communications, and transportation networks (Ferranti et al., 2017) highlighting the inter-dependencies of critical infrastructure. More recently, Storm Arwen in

2021 and Storm Eunice in 2022 have shown the continued need for resilient distribution infrastructure (BEIS, 2022a). Three categories of data are used for this analysis: historical distribution network fault information; historical weather data; and future climate projections. A summary showing the DNO service area and weather stations from which data were collected can be seen in Figure 1, with DNO boundaries obtained from (National Grid Electricity System Operator, 2020).

### 3.2 | Weather data

Meteorological data for the period January 1, 2001 through December 31, 2020 were taken from the MIDAS UK mean wind data set available from the Centre for Environmental Data Analysis (NCAS British Atmospheric Data Centre, 2021). Two variables are used: maximum wind gust and maximum wind gust direction. Maximum wind gust is used based on the underlying assumption that wind-related faults are caused by the highest wind speed in the hour surrounding the fault. Maximum wind gust direction is also used to explore the relationship with historical faults. Among the stations

proximal to the ENWL geographical area of responsibility, only stations with less than 10% missing data at hourly granularity were selected to maximize data quality. The stations were subsequently filtered to exclude stations above 250 m elevation as there is less power distribution infrastructure located at a higher elevation, and therefore wind speed and strength recorded at these higher elevations may be less representative of that experienced on the infrastructure network. This resulted in the removal of the Great Dun Fell (847 m) and Shap (252 m) stations. Hawarden Airport was also removed as it was farther south than the majority of faults. This resulted in seven weather stations for use: Blackpool Squires Gate, Crosby, Keswick, Rochdale, St. Bees Head, Walney Island and Warcop Range. Across the 20-year period, approximately 2% of hourly measurements are missing. Data is quality controlled by the Met Office, and therefore measurements with a version of ‘1’ are used indicating the Met Office’s “current best version” (Met Office, 2020). In addition, for this work, any duplicate measurement or hourly recording which did not contain a wind direction and wind gust measurement was removed. The climate was treated as stationary over the 20-year period evaluated, with the overall variation in maximum wind gusts over the period detailed in Section 4.1.

### 3.3 | Fault history

ENWL provided fault data for the period of July 1, 2001 to March 31, 2020. ENWL has approximately 7000–8000 km of overhead distribution lines (6.6/11 kV) and associated line equipment in the North West region of England, which are the focus of this case study. The service area can be seen in Figure 1. Data was obtained from ENWL’s fault database which is consistent with the information used to supply information to OFGEM’s National Fault Interruption Reporting Scheme (NAFIRS). Each record within the data set describes a fault that was logged in real time by ENWL operators and was subject to their internal data quality assurance procedures.

Along with the fault, an ENWL cause code records the best understanding of the fault’s origin. In this study, faults attributed to Wind and Gale (excluding windborne material) are selected resulting in 3860 faults after data cleaning. Each fault record also contains the fault location, a timestamp of when the fault occurred, the type of equipment that was affected, and the associated customer minutes lost (CML). An additional identifier is also included that indicates whether the fault was part of a major event (for example, Storm Desmond in 2015).

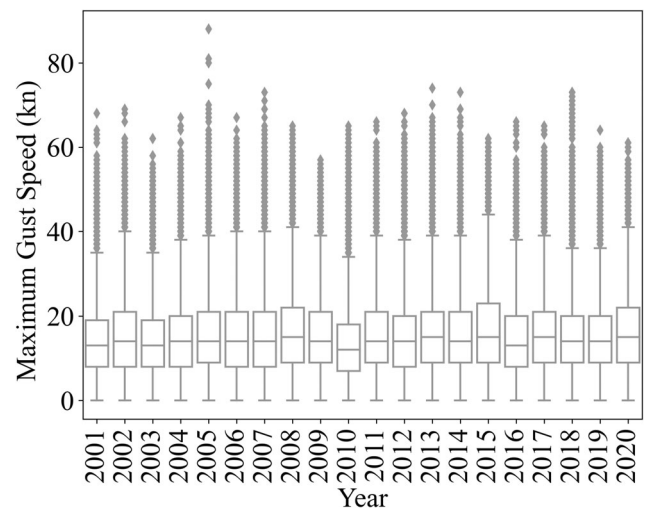


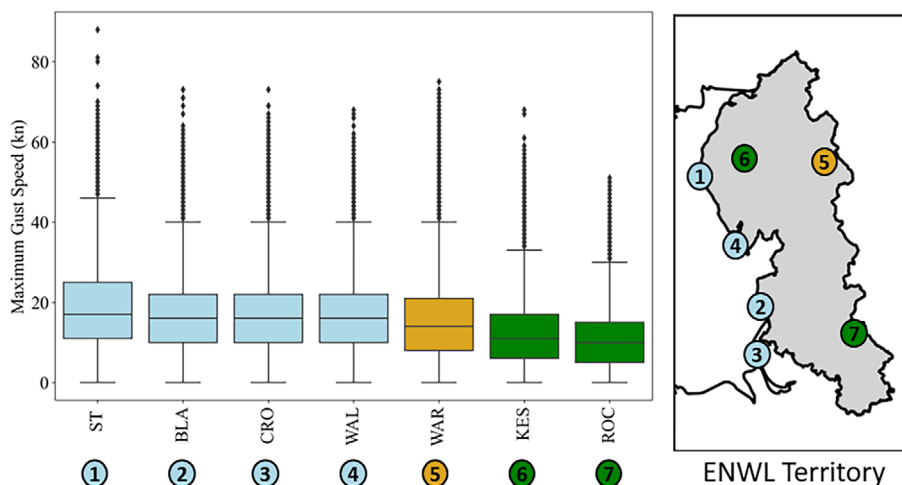
FIGURE 2 Variation in the maximum wind gust across the 20-year evaluation period.

As the faults are distributed throughout the service area, each fault was mapped to the nearest corresponding weather station based on proximity, with consideration given to their relative position to the central Cumbrian uplands. Mapping of the faults’ geo-location using the OS National grid to latitude/longitude was performed via the python OSGridConverter package (Porter, 2017) and distances were calculated using the geopy package (Karney, 2013). As one of the weather stations (Keswick) is adjacent to a mountainous area, faults that may be more proximal to Keswick, but are on the other side of the mountainous area (south of 54.5°) are instead assigned to Walney. As the granularity of available weather data improves in the future, a more refined mapping can be achieved. In order to account for the variation in the amount of electricity infrastructure in the area surrounding each of the weather stations, the length of overhead distribution lines is used as a normalizing factor. The total distance of the overhead conductor is first grouped by postcode and then the centroid of each postcode is mapped to the closest weather station.

## 4 | ANALYSIS

The methodology was implemented in python using: numpy (Harris, 2020), pandas (McKinney, 2010) and geopandas (Jordahl, 2021) packages for data processing; geopy (Karney, 2013), OSGridConverter (Porter, 2017) and shapely (Gillies, 2021) packages for geospatial analysis; matplotlib (Hunter, 2007), seaborn (Waskom, 2021) and cartopy (Elson, 2020) packages for visualization; and scipy (Virtanen, 2020) and statsmodels (Seabold, 2010) packages for statistical calculations.

**FIGURE 3** Regional differences in maximum wind gusts across stations in the study region. Colours used to indicate the three observed groups (coastal-blue, hilly-gold, inland-green).



#### 4.1 | Historical weather evaluation

Wind data for the region is compared to assess whether there is an observed change in maximum wind gusts over the 20-year study period (Figure 2). When inspecting the change of wind gust from 1 year to the next, a linear trend (fit using ordinary least squares) revealed an increase of 0.05 kn per year in the annual median value of maximum wind gust over the study period. As the magnitude of the annual change is relatively small and the regression coefficient was not significant ( $p = 0.109$ ), the historical maximum wind gust is treated as stationary for the purposes of this study.

Following the examination of the annual behaviour across the study area, the historical performance at each weather station was examined to identify the presence of regional variation. Examination of the weather station historical data reveals distinct differences between Coastal (St Bees Head, Walney, Blackpool, and Crosby), and Inland (Rochdale and Keswick) stations. The median maximum wind gust for each of these groups is 16.25 and 10.5 kn respectively. This differential of nearly 6 kn indicates clear geographic differences in wind profile. The Warcop station (hilly area) fell between these two groups with a median value of 14 kn but has high extreme values (Figure 3).

The last step of the historical weather evaluation was to calculate  $v_{\max}$  for each station to use in the normalization process. To avoid data sparsity in the historical measurements, a 5-year return period is used and the  $v_{\min}$  value for wind speed is set to 0. The process given in (3–7) is used to produce estimates of the magnitude of wind speed with a 5-year return interval for each of the seven weather stations. Table 1 shows the values of  $v_{\max}$  along with the coefficients. The resulting values of  $v_{\max}$  indicate the significant disparity in maximum wind gust

with a 24-kn difference between the two extremes (St. Bees Head and Rochdale). This evidences the substantial regional differences in wind loading.

#### 4.2 | Sub-regional fragility

To produce the fragility curve for each station, (1) is used in increments of 5 kn for each weather station area in the DNO territory. The maximum wind gusts for each station are grouped into bins of 5 kn (approximately 2.6 m/s) to minimize the impact of data sparsity which is more pronounced at higher wind gusts. This indicates how Figure 4 depicts these results. At low wind gusts all regions perform similarly, but from 35 kn and upwards, the points diverge. Based on historical data, faults are more likely in Rochdale at lower wind gusts, than in any other region, whereas failures are least likely in the Warcop Range region. While a single set of risk thresholds based on wind speed could be applied throughout the territory, Figure 4 indicates that using a single typical value would overestimate risk in some areas, while underestimating risk in others.

#### 4.3 | Sub-regional weather normalized fragility

To enable setting of consistent risk thresholds across an entire DNO area and compare vulnerability between the subregions, the fault rates can be normalized to the expected windspeeds seen in each region. Two design variables must be selected in order to produce the normalized fragility curve: the return period and bin size. As described above, the return period ( $v_T$ ) was selected to be 5 years for this case study. However, this value could be



Station name	Abbreviation	$U_{x'}$	$1/a_{x'}$	Maximum wind gust (kn)
St Bees Head	ST	3948	709	71
Warcop Range	WAR	3398	672	66
Crosby	CRO	3407	612	66
Blackpool Squires Gate	BLA	3199	600	64
Walney Island	WAL	3167	468	62
Keswick	KES	2627	521	58
Rochdale	ROC	1639	368	47

TABLE 1 Estimates of maximum annual wind gusts for each regional station (1-in-5 year return period).

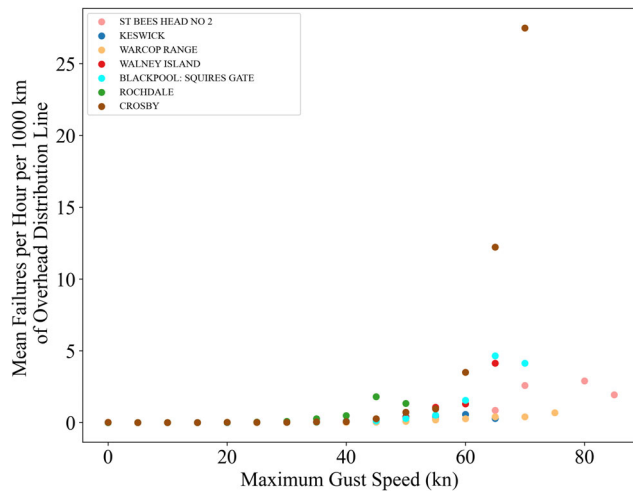


FIGURE 4 Historical faults for each sub-region demonstrating geospatial dispersion in risk.

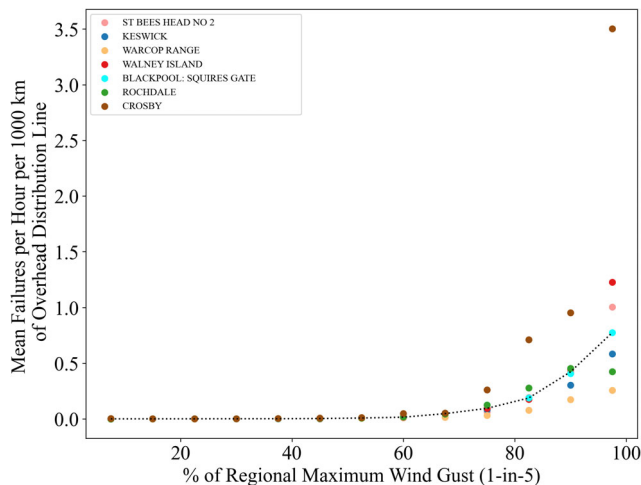


FIGURE 5 Normalized fragility curves for each region with the median value shown as a black dashed line.

varied to match the desired design criteria for a given set of assets. The median maximum wind gust across the stations with this return period was 64 kn. To approximate the same bin size used for Figure 4, the bin size was set to 7.5% as  $5/64$  is approximately 7.5%. The size of the bin

effects the number of historical measurements and should be scaled accordingly to ensure a sufficient sample size based on the number of stations being used. For this case study, each bin plotted contained 41 faults on average. The results can be seen in Figure 5. It can be observed that the risk of wind-related faults remains minimal below 60% of the regional maximum gust (similar to the regional fragility curves in Figure 4). This corresponds to nominal values ranging from 28 to 43 kn. However, even at higher windspeeds, there is much closer alignment across stations in the normalized fragility curves. Therefore, the normalized curves could be used to identify risk posed to the system in a spatially consistent fashion. While the variance between the regions is reduced in the normalized fragility curves, some difference remains. An example of this is the curve for Crosby, which is significantly higher than the other regions, or that of Warcop, which is lower than others. One potential reason for this could be local variance in observed wind speed. Although Crosby is closest in distance to many of the faults, it is located outside of the DNO area and is west of the observed faults. Other factors may also be involved that are not captured in the proposed normalized fragility curve and will be discussed further in Section 5. Dispersion is greatest in the final bin with wind speeds ranging from 97.5 to 100% of  $v_T$  and is excluded from the figure. The reason for this is that the probabilities in this bin are only based on a few hours and are much less robust. This further emphasizes the trade-offs between fragility curve granularity and bin size.

#### 4.4 | Variance in extreme winds across seasons and regime

The report regarding the recent behaviour of UK distribution infrastructure during Storm Arwen highlights the need for DNOs to consider other variables such as wind direction when anticipating the risk posed by extreme winds to the network (BEIS, 2022a). As the season and

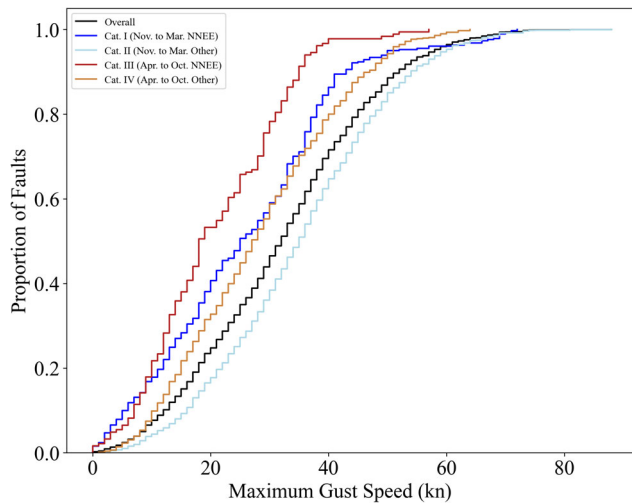


**FIGURE 6** Maximum Wind Gust Associated with Faults over Study Period ( $N = 381, 2504, 184, 791$ ).

wind direction are used to inform the current qualitative risk metrics employed by the DNO for this area, it is important to assess whether there is a change in maximum wind gust associated with faults across the categories used by the DNO. The four categories used for this work are Cat. I: Faults occurring November through March from the N/NE/E; Cat. II: Faults occurring November through March from other directions; Cat. III: Faults occurring April through October from the N/NE/E; and Cat. IV: Faults occurring April through October from other directions. A breakdown of the cumulative distribution function for each of the four categories can be seen in Figure 6. The figure shows that historically, faults in November through April (Cat. I and II) occur at higher wind speeds. Furthermore, across the year, faults from an N, NE, or E direction (NNEE) occur at lower wind speeds than those from other directions. There is also a disparity in the number of faults across categories with Cat. II containing more than 50% of faults. Therefore, the overall system wind speed profile for faults is most similar to this category. Because of the disparity in historical wind speeds associated with faults across these four categories, the use of a single Empirical Cumulative Distribution Function (ECDF) would reflect faults for Cat. II, but greatly overestimate the wind speeds associated with faults in other categories, most notably those in Cat. III.

Considerable variation across the season and wind direction can be observed. Three threshold quantiles are used to compare the historical wind gust associated with faults in each category (80%, 90%, and 95%). Comparing faults in Cat. I and II, the threshold points for faults from the N, NE or E are at 38, 43, and 50 kn respectively, whereas the thresholds increase to 48, 54, and 60 kn for

faults from other wind directions. This demonstrates there is a clear difference in faults associated with different wind regimes. Comparing the fault-inducing wind speeds across seasons also exhibits a marked difference with faults from November to March occurring at higher wind speeds when holding direction constant. Particularly more faults have occurred at lower wind speeds from April to October when the wind is from the N/NE/E and operators should plan to stand up emergency response actions at lower wind speeds during this period. Therefore, accounting for the changing sensitivity across seasons can be a beneficial means to further enhance the response to wind risk. These results indicate that there may be a further benefit for operators to differentiate the risk in a subregion by season and wind direction. However, even at a DNO level, there are a more limited number of observed faults in some periods such as Category III, which contained only 184 faults. As fragility curves are dependent on a sufficient quantity of historical data to produce robust outcomes, trade-offs between data quality and quantity must be balanced.

#### 4.5 | Study limitations

One of the most significant challenges when assessing fragility functions is the geospatial and temporal alignment of multivariate data. For example, the weather data is from seven stations throughout the DNO, but given the complex orography of the region, the wind speeds may vary significantly even a short distance apart. Therefore, more granular wind speed measurements could refine the accuracy of fragility functions. One way to remedy this could be through the installation of additional wind speed monitoring stations on or near pylons throughout the territory. Another example of challenges in alignment is the mapping of electrical assets to weather station zones. Further granularity of feeder-level infrastructure could improve the precision of the normalization. Another challenge is the amount of historical fault information in each bin used to develop the fragility curves. As the focus area becomes more granular, the number of faults decreases, leading to less robustness in the fragility function. When developing regional curves, consideration should be given to the sample size available for each curve. Grouping data in bins of 5 kn partially addresses this challenge, but at the tail values of wind speeds, only a few faults were recorded leading to the change in direction at extreme wind speeds for some stations. This effect is mitigated in the normalized fragility curve which does not include measurements beyond the 1-in-5-year maximum annual wind speed for each station. Lastly, it should be noted that the fragility curves

were calculated using 20 years of data and assumed stationary climate over this period. This assumption can be considered valid given the lack of a clear trend in maximum gust speed shown in Figure 2. Future enhancements to the accuracy of these curves may be provided through the incorporation of additional variables such as the age of assets, structural properties such as height tower type, material, etc., and surrounding land use and cover. With access to other variables, normalization could be conducted to account for the influence of these variables as well.

## 5 | IMPLICATIONS

### 5.1 | Operational response to severe weather

The DNO for the study area, ENWL currently employs a risk categorization to inform their operational response to severe weather events. There are four levels of risk (green, yellow, amber, red) and each elicits a different response to proactively prepare for outage events. The level of risk is a function of a wind gust, direction and season. Winds from the N, NE and E, are generally associated with failures at lower average wind speeds. From April to October, failures tend to occur at lower average wind speeds than during the rest of the year. Accordingly, the DNO applies the risk levels at different wind speeds for the four categories (Cat. I, II, III and IV) defined in Section 4.4. The risk levels and categories are derived and refined from learning from DNO experience of managing the network. This is in alignment with the finding from BEIS that DNOs should consider wind direction and speed in the setting of their alerts and preparation levels (BEIS, 2022b). By refining, the level of risk associated with different wind speeds across sub-regions the DNO may be able to further refine its operational preparation to manage the risk. This ensures a robust and effective use of resources across the business.

The value in continuous review of risk thresholds is the ability to better anticipate the damage caused by windstorms, allowing more accurate preparation of resources to improve overall system resilience. The DNO's operational response to risk initially involves four distinct parts of the business: control hub, local area operations, customer engagement and communications teams:

- *Control hub*: In the control hub, for a low-risk event, extra planners and dispatchers are mobilized to enable a simultaneous response to a growing number of incidents on the network. In more severe cases, a full incident management team (IMT) is mobilized along with

all available control engineers and outage technicians along with extra management support.

- *Local area operations*: In the local area, a similar structure of mobilization occurs. For low-risk warnings, an extra vegetation management team or line team may be mobilized along with placing extra crews on standby. For more severe events, this ramps up to include engineering support, line crews, vegetation teams and senior authorized engineers.
- *Customer engagement*: Customer engagement is also increased with corresponding increases in risk. At low levels, this may include placing customer service teams on standby, whereas for high risk this may include 24-h teams with all available inbound call takers. The customer engagement teams manage communications to customers through the website but also reach out to priority registered and vulnerable customers to offer proactive advice and support.
- *Communications*: The communications team actively manages and monitors all press queries and interest-pushing messages as appropriate to reassure customers, and at times of severe events, supports messages on social media and in news coverage. Social media is becoming increasingly essential to effective outage communication with its use by a variety of infrastructure operators.

As the scale of predicted events becomes increasingly severe so does the level and involvement of preparation across the business across all departments, contractors and levels of leadership.

### 5.2 | Implications for power DNOs

This study reveals key findings for ENWL, DNOs, and the sector more broadly. Firstly, the analysis of meteorological and fault data shows sub-regional differences in wind profile, and the relationship between wind strength and faults per 1000 km line length. Coastal regions experience higher maximum and average wind gusts (Figure 3) and have different relationships between line fault rate and maximum gust speed. For example, the inland region served by the weather station at Rochdale experiences higher fault rates at lower gust speeds. The reasons for this geospatial dispersion in risk are unclear; it may be related to historical variances in design standards or 'asset acclimatization' (i.e., assets located in areas of higher average wind speed are accustomed to a higher average wind speed; if not they would have already failed). Nonetheless, it emphasizes the benefit of considering a localized response to wind risk management that takes into account localized risk, and the

importance of using sub-regional weather data to inform operational risk management and asset management. Secondly, this study demonstrates that there are seasonal and directional components to the wind risk profile (Figure 6). It, therefore, provides a robust, quantitative underpinning for the current risk categories employed by the regional DNO, which are derived from their tacit experience of managing the network. Fragility curves provide a means of predicting the level of faults on a system for a particular wind speed and can provide a further numerical basis to derive different risk levels (e.g., green, amber, red) to support operational response. The analysis could be expanded to include other variables that ENWL uses to predict the impact on operational performance such as temperature or tree cover.

This analysis provides detailed evidence of the impact of wind on assets and outlines a robust methodological approach that may be applied to other weather impacts, such as extreme temperatures. Understanding the impact of current weather is a fundamental part of climate adaptation (Quinn et al., 2018). Moreover, under the 2008 Climate Change Act (2008), DNOs along with other infrastructure operators and organizations must report on the current and future impact of weather on their organization and their proposals to adapt to climate change under the Adaptation Reporting Power. The approach given here feeds into this process. Additionally, fragility curves could be linked with climate change projections to generate risk profiles for wind in future climate patterns (e.g., those found in Dobney et al. (2010)). For other DNOs, this study outlines an approach they may use to evaluate the risk that wind (or other variables) poses to their networks, and/or undertake a quantitative evaluation of their current risk management approach as the variance across sub-regions will differ from one DNO to the next. Having a clear understanding of the current impact of weather on infrastructure assets is imperative for effective operations as well as longer-term planning for climate resilience or vegetation management. Finally, this project shows the value of academic-practitioner knowledge exchange for the broader benefit of society and the economy. This project was co-created with ENWL to explore an operational issue within the context of climate change. Regular communications ensured the project outputs and outcomes remained fit for purpose. Effective knowledge exchange and project co-creation and co-implementation can ensure that publicly funded research benefits civil society.

### 5.3 | Implications in the wider context of climate change

Global mean temperature increase is changing regional climates, with a consequence for infrastructure assets

(Jaroszweski et al., 2021). For example, extreme weather may increase the frequency of weather impacts on a network, and/or may require assets to be designed for a different climate (e.g., with higher temperature extremes), and/or make some assets no longer viable (e.g., coastal infrastructure regularly inundated as a consequence of rising sea level) (Ranger et al., 2013). Within the UK, there are observed and projected trends towards milder, wetter winters and warmer summers, and hotter, drier summers, alongside an increase in the intensity of short-duration rainfall events (Met Office, 2019). However, for wind, the observational record shows no changes in storminess as measured by maximum gust speed (Fung et al., 2019). There is also limited observed change in maximum gust strength in the ENWL region during the 20-year period of this study (as shown in Figure 2). Global climate models from the UK Met Office (PPE-15) show an increase in near-surface wind speed during winter (December, January, February) from 1900 to 2100 (as compared from 1981 to 2000 averaging period); however, this increase is small compared with interannual variability and is not replicated by other climate models from the CMIP5 model intercomparison project (Fung et al., 2019). This increase in wind speed apparent within the PPE-15 model ensemble is linked to an increase in westerly weather types that bring westerly winds and mild wet conditions over the UK within the Met Office; again, this is not replicated in the CMIP5 model average (Maisey et al., 2019). This difference in projections of future wind strength is part of broader uncertainty surrounding the response of the North Atlantic jet stream strength and location (i.e., systematic changes in storm tracks) to a changing climate. Some models show the jet stream to be increasing in strength, while others do not; there is also no climate model consensus on the location of any changes (Shepherd, 2014, 2019).

It follows that in the future, the ENWL region may experience an increase in the frequency of weather events from the west, and may experience an increase in the mean wind speed affecting their assets but any change that may occur is small compared to interannual variability. For the DNO and infrastructure operators or organizers more broadly, this uncertainty surrounding future climate change projections has the potential to lead to inaction or maladaptation (Ranger et al., 2013). Instead, this uncertainty should be incorporated within the iterative process of climate change adaptation that should be part of business as usual (Quinn et al., 2018). DNOs should continue to record the impact of current weather on their assets, and periodically review information on climate change projections produced by organizations such as the Met Office. Asset management should take into account current and future weather impacts, and

design codes and standards may need to be modified to account for a changing climate. International Organization for Standardization standard ISO14090 *Adaptation to climate change* specifies principles, requirements and guidelines for organizations to adapt to climate change (ISO-14090:2019(en), 2019). As infrastructure is made more resilient in some areas, this may further increase the disparity in the regional fault risk, prompting the need for further evaluations of effective risk thresholds.

## 6 | CONCLUSIONS

This paper has combined historical fault data with meteorological information to understand the impact of wind on the infrastructure assets of a DNO located in north-west England. The analysis shows spatial variation in wind regimes and fault rates, within the broader influence that seasons and wind direction have on fault rate. The findings were discussed within the context of future projections of wind speed and strength under a changing climate, and within the policy context within the UK, which requires DNOs to understand and report on the impact of weather on their organization, and their efforts towards climate resilience.

The paper, therefore, has conceptual and practical value. Conceptually, it advances the use of fragility curves, by presenting normalized fragility curves that can facilitate a more ready comparison of power system infrastructure resilience across regions with varying climates. For industry, it describes an approach that any DNO may apply to understand the impact of weather on their systems, which can be used to inform operational response, evaluate existing operational response or provide the evidence base for long-term strategic decisions on asset management or climate adaptation. The electricity distribution network underpins other infrastructure networks including transport and ICT, and ensuring continuity of service is of national and international importance, now and in the future.

Looking forwards, future work should expand the analysis to examine the factors that may be contributing to spatial variation in performance, such as asset condition and design, maintenance regime, or land cover. Tree location and canopy size are particularly interesting when considering seasonal effects, and longer-term climate change, which may change tree species diversity and growing seasons; ultimately, a consequence of DNO vegetation management plans. Technological innovation may provide higher-resolution meteorological data or greater information on asset conditions. Therefore, methods to determine the fragility and risk of power distribution networks should be regularly examined.

## AUTHOR CONTRIBUTIONS

**Daniel L. Donaldson:** Conceptualization (equal); data curation (lead); formal analysis (lead); funding acquisition (supporting); methodology (lead); project administration (equal); writing – original draft (lead); writing – review and editing (lead). **Emma Ferranti:** Conceptualization (equal); data curation (supporting); formal analysis (supporting); funding acquisition (lead); methodology (supporting); project administration (equal); writing – original draft (lead); writing – review and editing (lead). **Andrew Quinn:** Formal analysis (supporting); methodology (supporting); writing – review and editing (supporting). **Dilan Jayaweera:** Conceptualization (supporting); funding acquisition (supporting); writing – review and editing (supporting). **Thomas Peasley:** Conceptualization (supporting); data curation (supporting); writing – review and editing (supporting). **Mark Mercer:** Conceptualization (supporting); methodology (supporting); writing – review and editing (supporting).

## FUNDING INFORMATION

The project was funded by an EPSRC Impact Acceleration grant awarded by the University of Birmingham. Emma Ferranti's time was co-funded by an EPSRC Fellowship grant, EP/R007365/1.

## ORCID

Daniel L. Donaldson  <https://orcid.org/0000-0003-3419-3624>

Emma J.S. Ferranti  <https://orcid.org/0000-0002-0494-5349>

Andrew D. Quinn  <https://orcid.org/0000-0003-0254-4661>

Dilan Jayaweera  <https://orcid.org/0000-0002-1009-9089>

## REFERENCES

- American Society of Civil Engineers. (2013) *Minimum design loads for buildings and other structures*, 7–10 edition. Reston, VA: American Society of Civil Engineers.
- BEIS. (2021) *Storm Arwen electricity distribution disruption review*. Available from: <https://www.gov.uk/government/publications/storm-arwen-electricity-distribution-disruption-review>.
- BEIS. (2022a) *Energy Emergencies Executive Committee Storm Arwen review: final report*. Available from: [https://assets.publishing.service.gov.uk/government/uploads/system/uploads/attachment\\_data/file/1081116/storm-arwen-review-final-report.pdf](https://assets.publishing.service.gov.uk/government/uploads/system/uploads/attachment_data/file/1081116/storm-arwen-review-final-report.pdf).
- BEIS. (2022b) *Energy Emergencies Executive Committee Storm Arwen Review: Interim Report*. Available from: [https://assets.publishing.service.gov.uk/government/uploads/system/uploads/attachment\\_data/file/1055504/arwen-review-interim-report.pdf](https://assets.publishing.service.gov.uk/government/uploads/system/uploads/attachment_data/file/1055504/arwen-review-interim-report.pdf).
- BSI. (2005) *Eurocode 1. Actions on structures. General actions. Wind actions*. BS EN 1991-1-4: 2005+ A1: 2010.

- Climate Change Act. (2008) *Climate Change Act c.27*. Available from: <http://www.legislation.gov.uk/ukpga/1999/28/contents>.
- Cook, N.J. (1985) *The designer's guide to wind loading of building structures*. London: Butterworth.
- Dobney, K., Baker, C.J., Chapman, L. & Quinn, A.D. (2010) The future cost to the United Kingdom's railway network of heat-related delays and buckles caused by the predicted increase in high summer temperatures owing to climate change. *Proceedings of the Institution of Mechanical Engineers, Part F: Journal of Rail and Rapid Transit*, 224(1), 25–34.
- Dunn, S., Wilkinson, S., Alderson, D., Fowler, H. & Galasso, C. (2018) Fragility curves for assessing the resilience of electricity networks constructed from an extensive fault database. *Natural Hazards Review*, 19(1), 04017019.
- Elson, P., Andrade, E.S.D., Hattersley, R., Campbell, E., May, R., Dawson, A. et al. (2020) SciTools/cartopy: Cartopy 0.18.0 (Version v0.18.0) [Computer software]. *Zenodo*. Available from: <https://doi.org/10.5281/ZENODO.3783894>
- ENWL. (2021) Climate change adaptation report, 2022. Stockport: Electricity North West Limited. Available from: <https://www.enwl.co.uk/globalassets/go-net-zero/net-zero/climate-change-adaption-report/2021---climate-change-adaptation-report.pdf>.
- Ferranti, E., Chapman, L. & Whyatt, D. (2017) A perfect storm? The collapse of Lancaster's critical infrastructure networks following intense rainfall on 4/5 December 2015. *Weather*, 72(1), 3–7.
- Fung, F., Bett, P., Maisey, P., Lowe, J., McSweeney, C., Mitchell, J. F.B. et al. (2019) *UKCP18 factsheet: weather types*. Available from: [https://www.metoffice.gov.uk/binaries/content/assets/metofficegovuk/pdf/research/ukcp/ukcp18-fact-sheet-wind\\_march21.pdf](https://www.metoffice.gov.uk/binaries/content/assets/metofficegovuk/pdf/research/ukcp/ukcp18-fact-sheet-wind_march21.pdf).
- Gillies, S., Taves, M., Arnott, J., Tonhofer, O., Van Den Bossche, J., Wasserman, J. et al. (2021) Toblerity/Shapely: Shapely 1.8.0 (Version 1.8.0) [Computer software]. *Zenodo*. Available from: <https://doi.org/10.5281/ZENODO.5597139>
- Gumbel, E.J. (1958) *Statistics of extremes*. New York, NY: Columbia University Press.
- Han, J., Kamber, M. & Pei, J. (2012) *Data mining: concepts and techniques*, 3rd edition. Waltham, MA: Morgan Kaufmann.
- Harris, C.R., Millman, K.J., van der Walt, S.J., Gommers, R., Virtanen, P., Cournapeau, D. et al. (2020) Array programming with NumPy. *Nature*, 585(7825), 357–362. Available from: <https://doi.org/10.1038/s41586-020-2649-2>
- Hunter, J.D. (2007) Matplotlib: a 2D graphics environment. *Computing in Science & Engineering*, 9(3), 90–95. Available from: <https://doi.org/10.1109/mcse.2007.55>
- IEEE. (2012) *IEEE guide for electric power distribution reliability indices*. IEEE Std 1366–2012 (Revision of IEEE Std 1366–2003), pp. 1–43.
- ISO-14090:2019(en). (2019) *Adaptation to climate change—principles, requirements and guidelines*. Standard ISO/TC 207/SC 7 TR 14090:2019. Geneva: International Organization for Standardization. Available from: <https://www.iso.org/standard/68507.html>.
- Jaroszweski, D., Wood, R. & Chapman, L. (2021) Infrastructure. In: Betts, R.A., Haward, A.B. & Pearson, V.K. (Eds.) *Third UK climate change risk assessment technical report*. London: Climate Change Committee.
- Jeong, S.-H. & Elnashai, A.S. (2007) Probabilistic fragility analysis parameterized by fundamental response quantities. *Engineering Structures*, 29, 1238–1251.
- Jordahl, K., Bossche, J.V.D., Fleischmann, M., McBride, J., Wasserman, J., Gerard, J. et al. (2021) Geopandas/geopandas: v0.9.0 (Version v0.9.0) [Computer software]. *Zenodo*. Available from: <https://doi.org/10.5281/ZENODO.4569086>
- Karney, C.F.F. (2013) Algorithms for geodesics. *Journal of Geodesy*, 87(1), 43–55. Available from: <https://doi.org/10.1007/s00190-012-0578-z>
- Lieblein, J. (1974) *Efficient methods of extreme-value methodology*. Technical Report NBSIR 74-602. Washington: National Bureau of Standards.
- Maisey, P., Thornton, H., Fung, F., Harris, G., Lowe, J., McSweeney, C. et al. (2019) *UKCP18 factsheet: weather types*. Available from: <https://www.metoffice.gov.uk/binaries/content/assets/metofficegovuk/pdf/research/ukcp/ukcp18-fact-sheet-weather-types.pdf>.
- McKinney, W. (2010) Data structures for statistical computing in Python. Proceedings of the 9th Python in Science Conference. <https://doi.org/10.25080/majora-92bf1922-00a>
- Met Office. (2014) *Winter storms*. Available from: <https://www.metoffice.gov.uk/binaries/content/assets/metofficegovuk/pdf/weather/learn-about/uk-past-events/interesting/2014/winter-storms-january-to-february-2014---met-office.pdf>.
- Met Office. (2016) *North West England and Isle of Man: climate*. Available from: [https://www.metoffice.gov.uk/binaries/content/assets/metofficegovuk/pdf/weather/learn-about/uk-past-events/regional-climates/north-west-england-isle-of-man\\_climate---met-office.pdf](https://www.metoffice.gov.uk/binaries/content/assets/metofficegovuk/pdf/weather/learn-about/uk-past-events/regional-climates/north-west-england-isle-of-man_climate---met-office.pdf) [Accessed: 6 July 2021].
- Met Office. (2019) *UK climate projections: Headline findings*. Available from: [https://www.metoffice.gov.uk/binaries/content/assets/metofficegovuk/pdf/research/ukcp/ukcp18\\_headline\\_findings\\_v3.pdf](https://www.metoffice.gov.uk/binaries/content/assets/metofficegovuk/pdf/research/ukcp/ukcp18_headline_findings_v3.pdf).
- Met Office. (2020) *MIDAS Data User Guide for UK Land Observations*. Available from: [http://cedadocs.ceda.ac.uk/1488/7/MIDAS\\_User\\_Guide\\_for\\_UK\\_Land\\_Observations\\_Version20200921.pdf](http://cedadocs.ceda.ac.uk/1488/7/MIDAS_User_Guide_for_UK_Land_Observations_Version20200921.pdf).
- Murray, K. & Bell, K.R.W. (2014) Wind related faults on the GB transmission network. *2014 International Conference on Probabilistic Methods Applied to Power Systems, PMAPS 2014-Conference Proceedings*, 11.
- National Grid Electricity System Operator. (2020) *GB DNO license areas 20200506 with ESRI shape file*. Available from: <https://data.nationalgrideso.com/system/gis-boundaries-for-gb-dno-license-areas>.
- NCAS British Atmospheric Data Centre. (2021) *MIDAS: UK mean wind data*. Available from: <https://catalogue.ceda.ac.uk/uuid/a1f65a362c26c9fa667d98c431a1ad38> [Accessed: 18 May 2021].
- Northern Powergrid. *Climate change adaptation report. Technical report*, 2010. Available from: <https://www.northernpowergrid.com/asset/0/document/194.pdf>.
- OFGEM. (2020) *RIIO-ED1 network performance summary 2019–2020*. Available from: [https://www.ofgem.gov.uk/sites/default/files/docs/2021/03/ed1\\_network\\_performance\\_summary\\_2019-20.pdf](https://www.ofgem.gov.uk/sites/default/files/docs/2021/03/ed1_network_performance_summary_2019-20.pdf).

- Palutikof, J.P., Brabson, B.B., Lister, D.H. & Adcock, S.T. (1999) A review of methods to calculate extreme wind speeds. *Meteorological Applications*, 6(2), 119–132.
- Panteli, M., Pickering, C., Wilkinson, S., Dawson, R. & Mancarella, P. (2017) Power system resilience to extreme weather: fragility modeling, probabilistic impact assessment, and adaptation measures. *IEEE Transactions on Power Systems*, 32(5), 3747–3757.
- Porter, J. (2017) *OSGridConverter 0.1.3*. Available from: <https://pypi.org/project/OSGridConverter/>.
- Quinn, A.D., Ferranti, E.J.S., Hodgkinson, S.P., Jack, A.C.R., Beckford, J. & Dora, J.M. (2018) Adaptation becoming business as usual: a framework for climate-change-ready transport infrastructure. *Infrastructures*, 3(2), 10.
- Ranger, N., Reeder, T. & Lowe, J. (2013) Addressing ‘deep’ uncertainty over long-term climate in major infrastructure projects: four innovations of the Thames Estuary 2100 Project. *EURO Journal on Decision Processes*, 1(3), 233–262.
- Schultz, M.T., Gouldby, B.P., Simm, J.D. & Wibowo, J.L. (2010) *Beyond the factor of safety: developing fragility curves to characterize system reliability geotechnical and structures laboratory*. Technical Report ERDC SR-10-1. Washington, DC: US Army Engineer Research and Development Center.
- Scott Hosking, J., MacLeod, D., Phillips, T., Holmes, C.R., Watson, P., Shuckburgh, E.F. et al. (2018) Changes in European wind energy generation potential within a 1.5°C warmer world. *Environmental Research Letters*, 13(5), 054032.
- Scottish and Southern Electricity Networks. (2021) *SSEN restores power to homes affected by Storm Arwen*. Available from: <https://www.ssen.co.uk/news-views/2021/2021-storm-arwen-red-alert/>.
- Seabold, S., & Perktold, J. (2010). Statsmodels: Econometric and statistical modeling with Python. In *Proceedings of the 9th Python in Science Conference* (Vol. 57, No. 61, pp. 10–25080).
- Shepherd, T.G. (2014) Atmospheric circulation as a source of uncertainty in climate change projections. *Nature Geoscience*, 7(10), 703–708.
- Shepherd, T.G. (2019) Storyline approach to the construction of regional climate change information. *Proceedings of the Royal Society A*, 475(2225), 20190013.
- Shield, S.A., Quiring, S.M., Pino, J.V. & Buckstaff, K. (2021) Major impacts of weather events on the electrical power delivery system in the United States. *Energy*, 218, 3.
- Tomas Lagos, Rodrigo Moreno, Alejandro Navarro Espinosa, Mathaios Panteli, Rafael Sacaan, Fernando Ordonez, Hugh Rudnick, and Pierluigi Mancarella. Identifying optimal portfolios of resilient network investments against natural hazards, with applications to earthquakes. *IEEE Transactions on Power Systems*, 35(2):1411–1421, 3 2020.
- Troshka, L. (2022) *NIA project annual progress report document—assessment of climate change event likelihood embedded in risk assessment targeting electricity distribution (ACCELERATED)*, 6. Available from: <https://www.nationalgrid.co.uk/downloads-view-reciteme/596752> [Accessed: 30 January 2023].
- Virtanen, P., Gommers, R., Oliphant, T.E., Haberland, M., Reddy, T., Cournapeau, D. et al. (2020) SciPy 1.0: fundamental algorithms for scientific computing in Python. *Nature Methods*, 17(3), 261–272. Available from: <https://doi.org/10.1038/s41592-019-0686-2>
- Waskom, M. (2021) Seaborn: statistical data visualization. *Journal of Open Source Software*, 6(60), 3021. Available from: <https://doi.org/10.21105/joss.03021>
- Wilkinson, S., Dunn, S., Adams, R., Kirchner-Bossi, N., Fowler, H. J., Otálora, S.G. et al. (2022) Consequence forecasting: a rational framework for predicting the consequences of approaching storms. *Climate Risk Management*, 35, 100412.
- Zareei, S.A., Hosseini, M. & Ghafory-Ashtiany, M. (2016) Seismic failure probability of a 400kV power transformer using analytical fragility curves. *Engineering Failure Analysis*, 70, 273–289.

**How to cite this article:** Donaldson, D. L., Ferranti, E. J.S., Quinn, A. D., Jayaweera, D., Peasley, T., & Mercer, M. (2023). Enhancing power distribution network operational resilience to extreme wind events. *Meteorological Applications*, 30(2), e2127. <https://doi.org/10.1002/met.2127>